ULTRASONIC TECHNIQUES FOR CHARACTERIZATION OF MANUFACTURING DEFECTS IN THICK COMPOSITES

I. M. Daniel and S. C. Wooh
Technological Institute
Northwestern University
Evanston, IL 60208

INTRODUCTION

New structural applications of polymer matrix composites require the use of thick sections. The fabrication and use of such thick sections create new needs for flaw detection and characterization which cannot be met adequately by conventional nondestructive evaluation (NDE). These composites are susceptible to manufacturing defects due to thermal gradients and nonuniform resin bleeding during curing.

Typical processing defects in thick composites include matrix cracks, delaminations, porosity and non-uniform matrix distribution. These defects can be further aggravated by service loading, such as impact and thermomechanical loading.

A variety of NDE techniques are used for evaluating the integrity of composite materials. Various methods are best suited for detecting different types of flaws. The most effective and practical methods are the ultrasonic and radiographic methods. These methods can be supplemented by others, such as acoustic emission, interferometric, and wave propagation techniques. Although ultrasonic methods have some limitations related to attenuation and penetration, they still offer the most promising approach to NDE of thick composites.

EXPERIMENTAL PROCEDURES

The material investigated was AS4/3501-6 graphite/epoxy (Hercules, Inc.). It was obtained in prepreg form and was fabricated into 10.16 cm x 15.24 cm (4 in. x 6 in.) unidirectional 200-ply thick plates. The thickness of these plates was approximately 2.5 cm (1 in.). Specimens were prepared with four types of defects: (1) Embedded Teflon inclusions; (2) interlaminar grease spots; (3) fiber fractures; and (4) porosity.

Conventional pulse echo techniques using a focused transducer are not suitable in these cases and must be modified and enhanced. A modified through-transmission technique employing an unfocused transmitting transducer and a focused receiving transducer [1]. The receiving transducer was focused on the back surface of the specimen to detect the shadow of the defect. These transducers were 5 MHz broad-band transducers of 1.90 cm (0.75 in.) diameter. The receiving transducer had a focal length of 5.08 cm (2 in.).

The RF signal received by the receiving transducer was fed through a gated peak detector. The output peak voltage was recorded by a low speed A/D converter (HP 7090A) and transmitted to a micro-computer (IBM PC/AT). The movement of the scanning bridge with the transducers was programmed by the micro-computer. The peak voltage recorded was considered as an image function or grey scale of the spatial coordinates, $f(x, y)$. The continuous function $f(x, y)$ was approximated by an equally spaced array of discrete samples. A moderate resolution of 256 × 256 array of pixels and 256 grey levels was used. Thus a grey-level image depicting a planar view of the specimen with its defects was obtained.

In most cases the as obtained image was somewhat blurry and degraded. For this reason enhancement techniques were applied to enhance and restore the fidelity of the image [2]. Enhancement techniques used include histogram equalization, thresholding, log operation and contrast stretching. No single enhancement technique was optimum in all cases. A suitable combination of techniques was selected for optimum image quality.

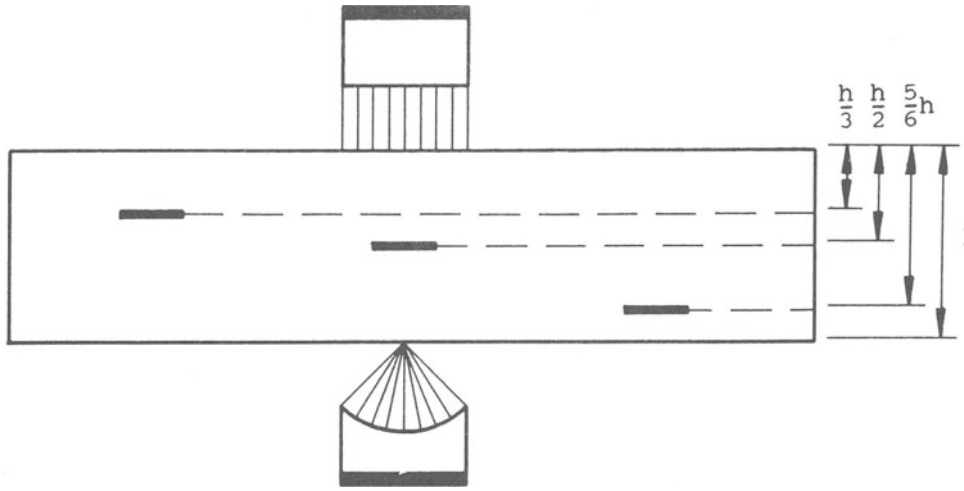

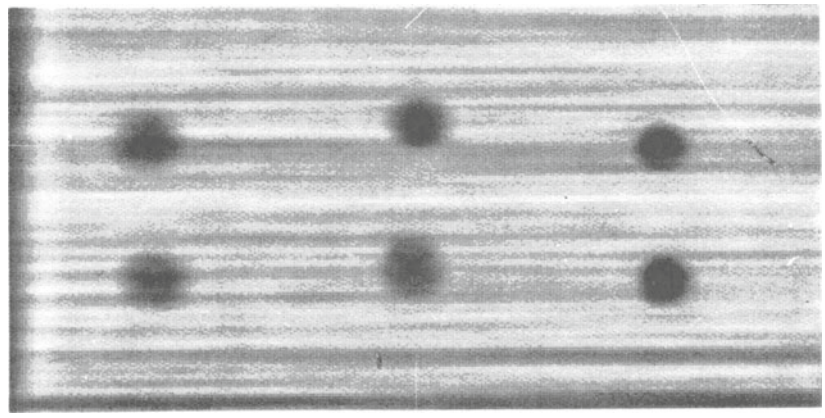

Fig. 1. Through Transmission C-Scan of 150-Ply Graphite/Epoxy Laminate with Embedded 7.9 mm (0.31 in.) diam., 0.025 mm (0.001 in.) Thick Inclusion, before Enhancement.

RESULTS AND DISCUSSION

Embedded Teflon Inclusions

This specimen was a 150-ply thick unidirectional graphite/epoxy plate with 7.9 mm (0.31 in.) diameter and 0.025 mm (0.001 in.) thick Teflon inclusions. These inclusions were embedded between the plies as various locations through the thickness.

The as obtained C-scan obtained by the through-transmission technique discussed before is shown in Fig. 1. The image seems blurry and the edges of the embedded inclusions are not well defined. The grey scale variation along an axis through three of the inclusions is shown in Fig. 2. The low contrast and definition seen is related to the somewhat gradual change in grey scale across the inclusions boundary.

In order to enhance the contrast, the histogram equalization technique was used first [3]. From the frequency distribution of each grey value in the image, the grey scale histogram can be obtained as a global description of the quality of the picture. The histogram equalization technique uses a transformation function such that each grey level has approximately the same number of pixel elements. Each grey level value z, normalized to lie in the [0,1] range, is replaced by its cumulative distribution function

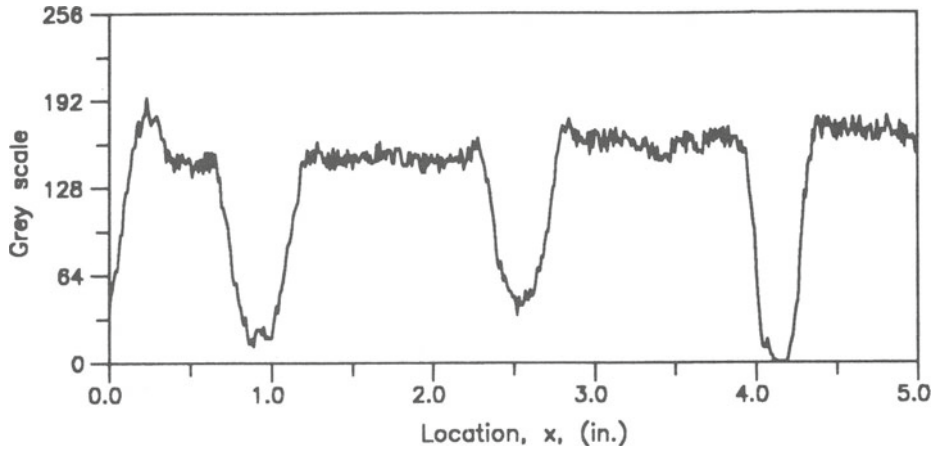

Fig. 2. Ultrasonic Through-Transmission Along Section through Inclusions. (Original Scan)

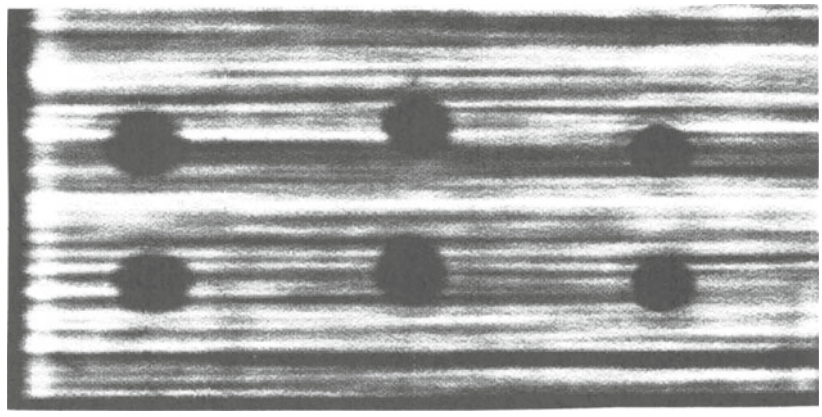

Fig. 3. C-Scan of Specimen with Embedded Inclusions after Histogram Equalization.

$$z' = \int_0^z p_z(\xi)d\xi \qquad 0 \le z \le 1 \tag{1}$$

where $p_z(z)$ is the probability density function. This transformation will produce a nearly flat histogram, representing that the frequency of appearance of each grey value is the same.

In discrete representation the probability density function is approximated by

$$p_z(z_k) = \frac{n_k}{n} \qquad 0 \le z_k \le 1 \qquad (k = 0, 1, \cdots, L-1) \tag{2}$$

where L is the total number of grey levels (256 in this case), $p_z(z_k)$ is the probability of appearance of the kth grey level, n_k is the number of times this level appears in the image, and n is the total number of pixels in the image. In this case the transformation function, i.e., the cumulative distribution function, is given by

$$z_k' = \sum_{j=0}^{k} \frac{n_j}{n} \tag{3}$$

This technique results in the overall improvement of contrast as seen in Fig. 3. However, it may not always preserve dimensional fidelity.

Another enhancement technique combining thresholding, logarithmic transformation and contrast stretching proved more effective in this case. In the thresholding operation the pixel values are remapped to other values under a given threshold criterion. Given the original image function $f(x, y)$, the thresholded output between 0 and T is given by

$$\text{thresh}[f(x,y)] = \begin{cases} f(x,y) & \text{if } f(x,y) \le T \\ T & \text{if } f(x,y) > T \end{cases} \tag{4}$$

This operation eliminates any spurious spikes caused by instrumentation noise or particles in the immersion tank.

A further operation is performed, the so-called logarithmic operation, defined as follows:

$$L(x,y) = \log[1 + \text{thresh}(f(x,y))] \tag{5}$$

Finally, a contrast stretch transformation is performed on the result above as follows:

$$g(x,y) = \text{stretch}[L(x,y)] = a + \frac{b-a}{q-p}[L(x,y) - p] \tag{6}$$

where

$p = \min[L(x,y)]$
$q = \max[L(x,y)]$
$[a,b]$ = range of available grey values

The result of the series of transformations described by eqs. (4), (5) and (6) is shown in the grey level variation along an axis through the inclusions (Fig. 4) and in the enhanced image of Fig. 5.

Embedded Grease Spots

This specimen was a 200-ply thick unidirectional graphite/epoxy plate with silicon grease spots placed between plies during lamination (Fig. 6). Furthermore, because of resin bleeding along the two short edges normal to the fibers, a region of variable porosity developed in the central part of the specimen.

The initially obtained image was enhanced by a combination of thresholding, logarithmic transformation and stretching as shown in Fig. 7. This enhancement delineates the grease spots and the porous area very clearly but it does not provide a quantitative characterization of porosity.

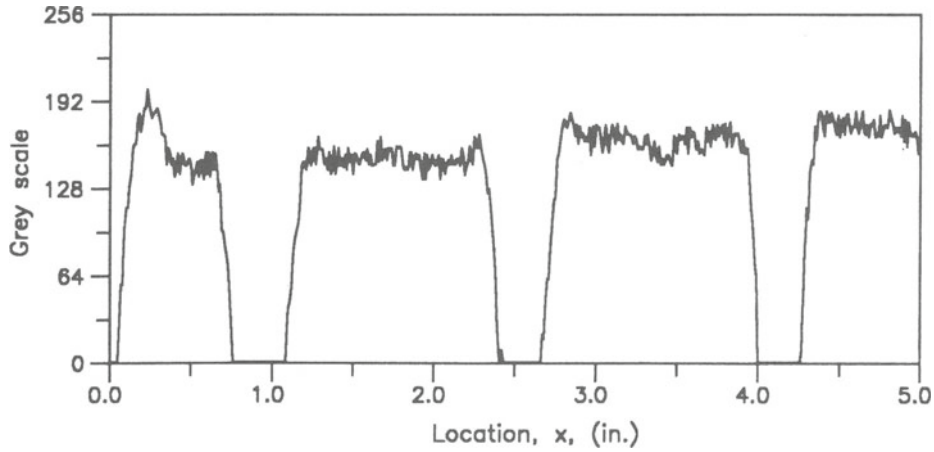

Fig. 4. Ultrasonic Through-Transmission along Section through Inclusions. (Scan after Thresholding, Log Operation, and Stretching)

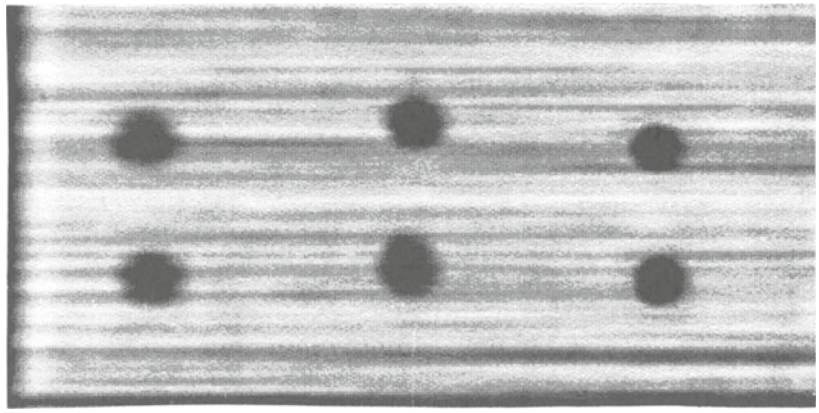

Fig. 5. C-Scan of Specimen with Embedded Inclusions after Enhancement by Thresholding, Log Operation and Stretching.

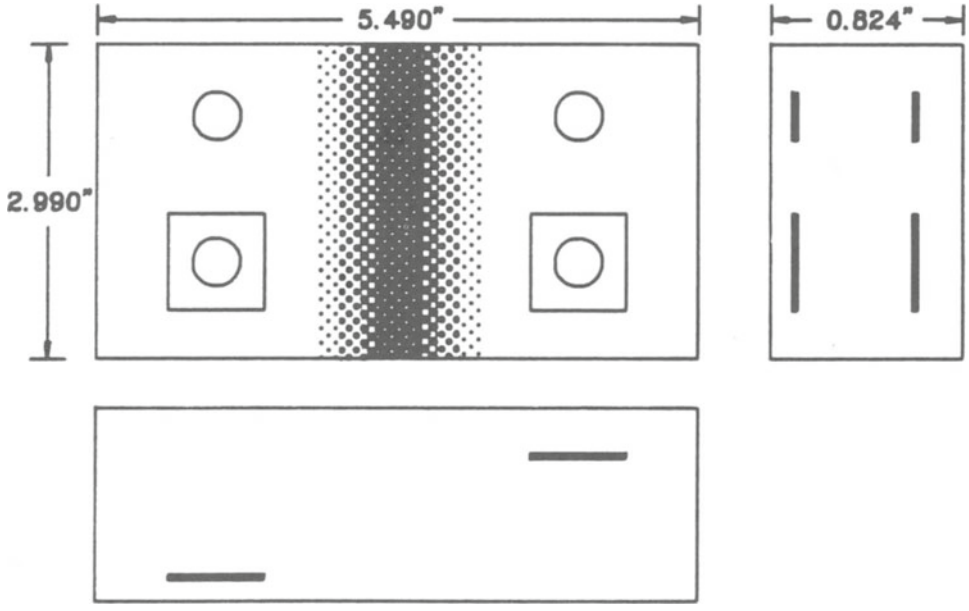

Fig. 6. Unidirectional 200-Ply Graphite/Epoxy Laminate with Embedded Grease Spots and Porosity.

Fiber Fractures

This specimen was a 200-ply thick unidirectional graphite/epoxy plate where the fibers of 8 to 10 consecutive plies were cut prior to fabrication. This resulted in appreciable movement of the segments of the cluster of broken plies, with the gaps filled by matrix and material from the unbroken plies. A region of variable porosity also developed in the center of the specimen as in the case before.

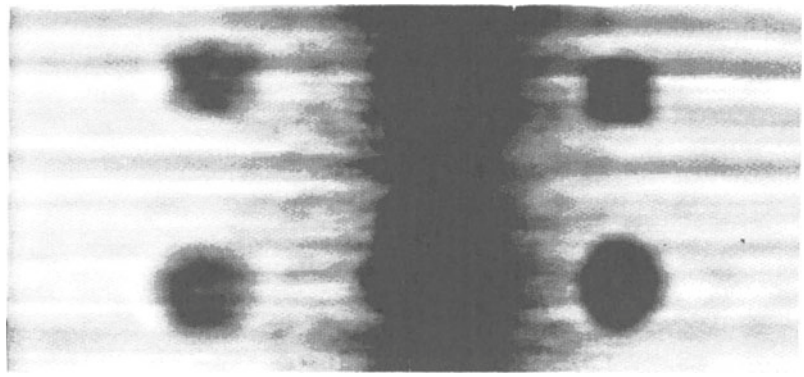

Fig. 7. C-Scan of Specimen with Embedded Grease Spots and Porosity after Enhancement by Thresholding, Log Operation, and Stretching.

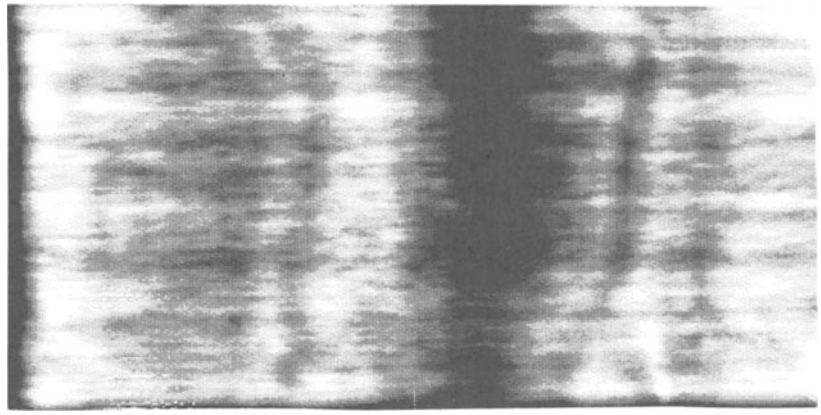

Fig. 8. C-Scan of Specimen with Broken Fibers and Porosity after Enhancement by Thresholding, Log Operation, and Stretching.

The C-scan image was enhanced by a combination of thresholding, logarithmic transformation and stretching as shown in Fig. 8. The ends of the broken cluster of plies as well as the porous region in the center are visible in the image.

Porosity

Appreciable porosity developed in the central region of both specimens discussed before. This porosity reaches its peak value at the center and decreases rapidly with distance from the center along the longitudinal centerline. The quantitative nondestructive characterization of this porosity is a challenging problem.

The variation of grey scale or ultrasonic through-transmission along the longitudinal axis shows a qualitative correlation between grey level and expected degree of porosity (Fig. 9). The quantify this correlation it is necessary to measure the degree of porosity and its variation destructively. Four locations along the axis were selected for quantitative destructive measurements. Small coupons were machined from the specimen along the longitudinal axis with one of their faces located at distances of 0 mm, 7.1 mm (0.28 in.), 150 mm (0.59 in.) and 22.1 mm (0.87 in.) from the center. These faces were polished and examined microscopically. Typical photomicrographs taken along the centerline of the specimen are shown in Fig. 10. Porosity takes the form of elongated voids randomly distributed. It varied both through the thickness and along the longitudinal axis. Five such

photomicrographs at various locations through the thickness were analyzed for each axial location. The average through-the-thickness porosity thus measured and plotted versus the measured grey scale or transmission coefficient in Fig. 11. The porosity decreases from approximately 1% at the center of the specimen to nearly zero at a distance of 2.54 cm (1 in.) from the center. The porosity versus grey scale curve, if it is proven reproducible for a certain group of specimens can serve as a calibration curve for quantitative nondestructive determination of average porosity.

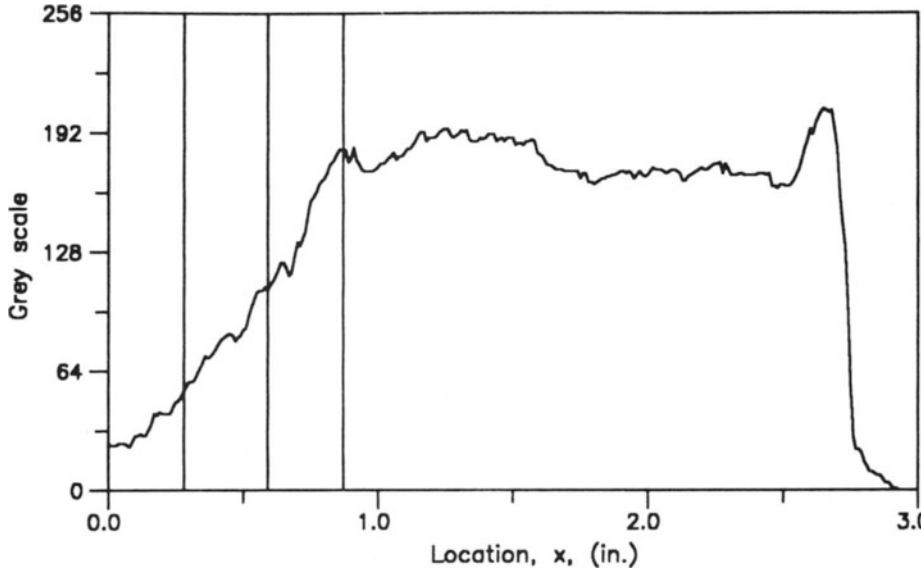

Fig. 9. Ultrasonic Through-Transmission along Longitudinal Centerline with Locations of Subsequent Porosity Measurement.

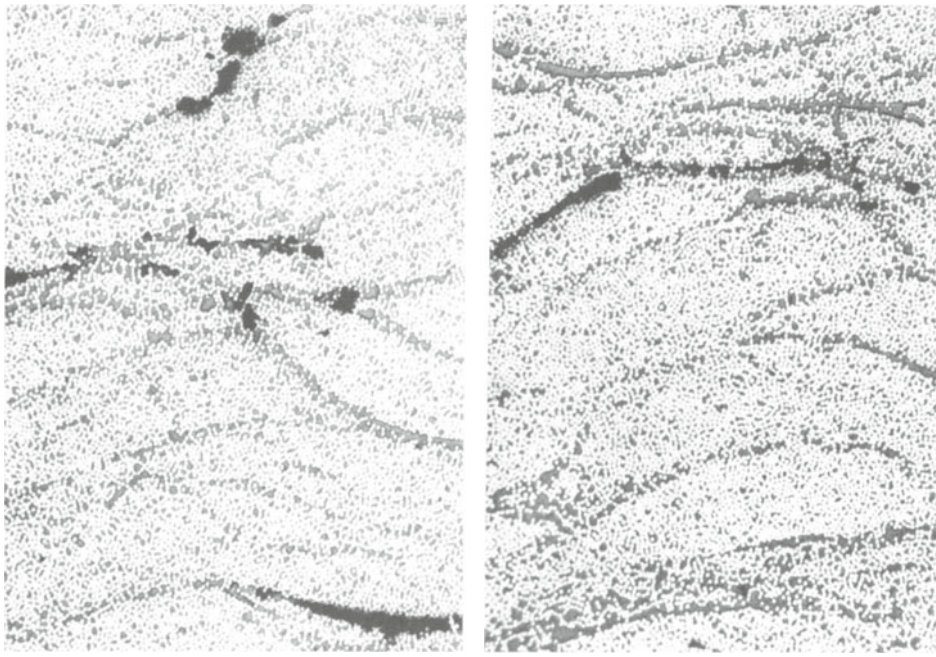

Fig. 10. Transverse Cross Section of Composite Specimen Showing Porosity. (Center of Specimen)

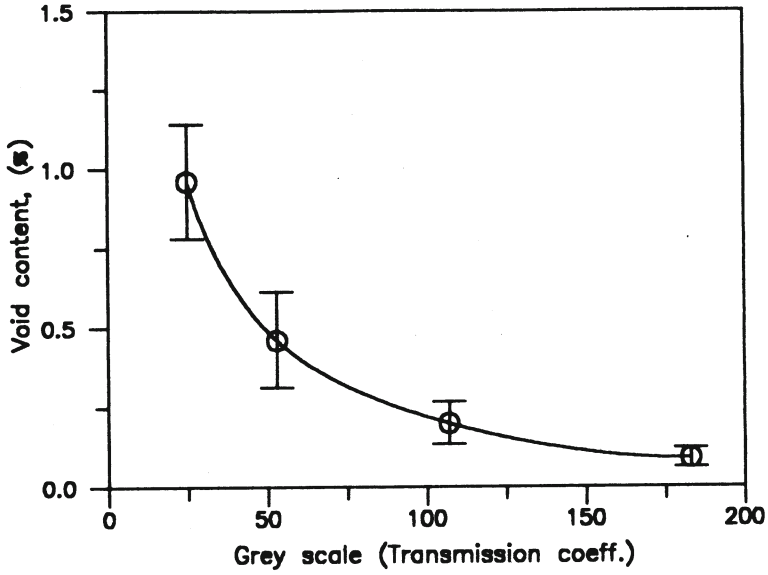

Fig. 11. Correlation of Average Porosity and Ultrasonic Transmission along Longitudinal Centerline.

SUMMARY AND CONCLUSIONS

Ultrasonic techniques were developed and applied for detection and characterization of manufacturing defects in thick composites. Graphite/epoxy specimens, 150- and 200-ply thick, were prepared with four types of defects: embedded Teflon inclusions, interlaminar grease spots, fiber fractures and porosity. A through-transmission technique employing an unfocused transmitting and a focused receiving transducer was found suitable for thick composites.

Enhancement techniques were used to improve the initially obtained images of these, histogram equalization while it improves contrast may not preserve dimensional fidelity. Best results were obtained by a combination of thresholding, logarithmic transformation and contrast stretching.

The definition and sharpness of the acoustic image increases as the feature/defect gets closer to the receiving focused transducer. This was the case for the embedded inclusions and grease spots. Fiber fracture and ply separation were detected by the techniques used. Porosity averaged through the thickness was correlated with average density and ultrasonic transmission, thus showing the potential for quantitative nondestructive determination of porosity in thick composites.

ACKNOWLEDGEMENTS

The work described here was sponsored by the Office of Naval Research. We are grateful to Dr. Y. Rajapakse of ONR for his encouragement and cooperation and to Mrs. Yolande Mallian for typing this manuscript.

REFERENCES

1. I. M. Daniel, S. C. Wooh and J. W. Lee, "Defect and Damage Characterization in Composite Materials," Review of Progress in Quantitative Nondestructive Evaluation, Vol. 6B, ed. by Donald O. Thompson and Dale E. Chimenti, Plenum Publishing Corp., 1987, pp. 1195-1202.
2. S. C. Wooh and I. M. Daniel, "Enhancement Techniques for Ultrasonic Imaging of Damage in Composite Materials," New Directions in the Nondestructive Evaluation of Advanced Materials, ASME Winter Annual Meeting, Nov. 28-Dec. 2, 1988, Chicago, IL.
3. R. C. Gonzalez and P. Wintz, Digital Image Processing, Addison-Wesley Publishing Co., Reading, MA, 1977.